The Canadian Mineralogist
Vol. 57, pp. 489-498 (2019)
DOI: 10.3749/canmin.1900012

JERVISITE, $NaScSi_2O_6$: OPTICAL DATA, MORPHOLOGY, RAMAN SPECTROSCOPY, AND CRYSTAL CHEMISTRY

PIETRO VIGNOLA[§]

CNR-Istituto per la dinamica dei processi ambientali, via Mario Bianco, 9, I-20131 Milano, Italia

NICOLA ROTIROTI

Dipartimento di Scienze della Terra, Università degli Studi di Milano, via Botticelli 23, I-20133 Milano, Italia

FRÉDÉRIC HATERT

Laboratoire de Minéralogie, Département de Géologie, Université de Liège, Bâtiment B18, Sart Tilman, B-4000 Liège, Belgique

DANILO BERSANI

Dipartimento di Scienze Matematiche, Fisiche e Informatiche, Università di Parma, Parco Area della Scienza 7/a, 43124 Parma, Italia

SERGIO ANDÒ

Dipartimento di Scienze dell'Ambiente e della Terra (DISAT), Università di Milano-Bicocca, Piazzale della Scienza 4, 20126 Milano, Italia

SERGIO VARVELLO

Vai De Vit 17 – 28838, Stresa, Italia

ABSTRACT

The crystal structure of jervisite, ideally $NaScSi_2O_6$, was refined using single-crystal X-ray data collected using a crystal from the Seula quarry (Baveno, Verbano-Cusio-Ossola province, Italy). The refinement was carried out in the *C*2/*c* space group giving the following unit-cell dimensions: $a = 9.8478(2)$ Å, $b = 9.0575(1)$ Å, $c = 5.3409(3)$ Å, $\beta = 106.87(2)°$, and $V = 455.89(2)$ Å^3 for $Z = 4$. The previous crystal structure, refined using data from a synthetic analogue and a natural sample, was confirmed and conforms with that of aegirine. The bond-valence calculation and the refined occupancy of the *M*1 and *M*2 sites confirm the cation distribution adopted in the empirical formula. Raman spectroscopy and refractive index measurements were also performed, and the morphology was studied in order to provide a complete description of this Sc-bearing Na pyroxene.

Keywords: jervisite, crystal structure, single-crystal X-ray diffraction, electron microprobe, Raman spectroscopy, Gladstone-Dale index, Baveno, Italy.

INTRODUCTION

The miarolitic NYF pegmatites hosted by the calc-alkaline Baveno pluton contain an important Sc-minerals association. Indeed, six of the 19 known scandium mineral species occur as fine crystals in the cavities of the Baveno granite. Bazzite, $Be_3Sc_2(Si_6O_{18})$, was the first scandium mineral found and

§ *Corresponding author e-mail address*: pietro.vignola@idpa.cnr.it, pietroevignola@gmail.com

FIG. 1. Divergent group of prismatic jervisite crystals measuring up to 300 μm from the Seula quarry.

described from Baveno (Artini 1915, Demartin *et al.* 2000). Baveno is also the type locality for cascandite, $CaScSi_3O_8(OH)$, scandiobabingtonite, $(Ca,Na)_2(Fe^{2+},Mn)(Sc,Fe^{3+})Si_5O_{14}(OH)$, and jervisite (Orlandi *et al.* 1998, Mellini *et al.* 1982). Thorveitite, $Sc_2Si_2O_7$, was reported by Orlandi (1990) and Gramaccioli *et al.* (2004). Kristiansenite, $Ca_2ScSn(Si_2O_7)(Si_2O_6OH)$, is the most recent scandium mineral to be identified from Baveno (Guastoni & Pezzotta 2004).

Jervisite, $NaSc^{3+}Si_2O_6$, was discovered in the pegmatitic dikes hosted by the Baveno granitic pluton in Piedmont, Italy (Mellini *et al.* 1982). The only other locality for jervisite is the Deadhorse Creek deposit, Walsh, Thunder Bay district in Ontario, Canada, where it occurs as micro-prisms up to 50 μm hosted by quartz in a volcanic breccia associated with Sc-rich pyroxene (Potter & Mitchell 2005). The jervisite at Baveno was described by Mellini *et al.* (1982) as platy, light green minute crystals associated with pink cascandite, found at the Giacomini quarry, near the village of Agrano, Omegna municipality, Verbano-Cusio-Ossola province. The crystal structure of jervisite could not be determined in the original study due to the low amount and low quality of crystals available and the intimate intergrowth with cascandite, $CaScSi_3O_8(OH)$, the scandium analogue of pectolite and serandite (Mellini *et al.* 1982). However, a powder pattern obtained using a Gandolfi camera demonstrated that jervisite has the same crystallographic character as a synthetic analogue of aegirine, $NaFe^{3+}Si_2O_6$, which was synthesized by Ito & Frondel (1968) and whose structure was solved by Hawthorne & Grundy (1973). Recently, Merlino & Orlandi (2006) refined the crystal structure of jervisite using a sample from the Prini quarry (Baveno), finding a very good agreement with the crystal structure refined by Hawthorne & Grundy (1973) using data from the synthetic analogue. A recent find of crystals of jervisite of exceptional quality (Fig. 1) allowed new chemical, optical, morphological, and structural investigations and made possible the complete description of jervisite from the optical and crystal-chemical point of view.

BACKGROUND INFORMATION

The original chemical data for jervisite from Mellini *et al.* (1982) are reported in Table 1. These were used to write the simplified chemical formula $(Na,Ca,Fe^{2+})(Sc,Mn,Fe^{2+})Si_2O_6$, from which the ideal

TABLE 1. ELECTRON MICROPROBE COMPOSITION OF THE INVESTIGATED JERVISITE CRYSTAL AND COMPARISON WITH LITERATURE VALUES

	wt.%	wt.%	wt.%§	esd§		ion *apfu**		
	1	2	3			1	2	3
SiO_2	50.42	52.17	53.75	0.39	Si	2.000	2.000	2.000
TiO_2	0.55	0.31	0.17	0.03	Ti	0.016	0.009	0.005
Al_2O_3	0.42	0.4	0.32	0.06	Al	0.020	0.018	0.014
Sc_2O_3	18.48	25.62	26.83	1.34	Sc	0.639	0.856	0.870
FeO	8.59	2.58	2.28	0.76	Fe^{2+}	0.285	0.083	0.071
MnO	0.44	1.24	1.32	0.50	Mn	0.015	0.040	0.042
MgO	2.8	0.54	0.05	0.02	Mg	0.166	0.031	0.003
CaO	7.25	4.27	3.40	0.95	Ca	0.308	0.175	0.136
Na_2O	5.55	10.62	11.50	0.62	Na	0.427	0.789	0.830
Total	94.5	97.75	99.62		O^{2-}	6.007	6.053	6.001

Notes: § average of seven spots; * *apfu* normalized considering 2 Si *apfu*; (1) data from Mellini *et al.* (1982); (2) data from Merlino & Orlandi (2006); (3) present study.

formula $NaSc^{3+}Si_2O_6$ was derived (Mellini *et al.* 1982). Chemical and crystallographic information were used to classify jervisite as a Sc-bearing pyroxene belonging to the aegirine–augite series. The unit-cell parameters refined from the powder pattern in space group *C*2/*c* were $a = 9.853(11)$ Å, $b = 9.042(10)$ Å, $c = 5.312(7)$ Å, $\beta = 106.37(7)°$, in good agreement with those previously measured from the synthetic analogue: $a = 9.8438(4)$ Å, $b = 9.0439(4)$ Å, $c = 5.3540(2)$ Å, $\beta = 107.215(2)°$ (Hawthorne & Grundy 1973). The crystal structure of the synthetic analogue, as can be inferred from the data of Hawthorne & Grundy (1973), corresponds to that of sodic pyroxenes in which the *M*1 site is a distorted octahedron occupied mainly by Sc, and the *M*2 site, a distorted eight-folded antiprism, is occupied mainly by Na. Merlino & Orlandi (2006) confirmed the crystal structure previously described by Hawthorne & Grundy (1973) with unit cell parameters $a = 9.844(2)$ Å, $b = 9.059(2)$ Å, $c = 5.328(2)$ Å, $\beta = 106.55(2)°$. The general topology of pyroxene-group minerals is confirmed for jervisite. As in all pyroxenes, the *M*1 and *M*2 sites form two chains parallel to **c**. The chain of octahedra occupied by Sc are linked by edge sharing, whereas the chain of Na-centered polyhedra links on [001] by corner sharing. Both types of chain alternate along [010] to form layers in the **b–c** plane. The SiO_4 tetrahedra form chains parallel to the **c** axis by sharing two of the four corners. The Si chains are bonded to the layer formed by the *M*1 and *M*2 sites, giving the lattice of the pyroxene (Fig. 2 and 3).

After its initial description jervisite was also found in the other quarries belonging to the Baveno municipality and close to the villages of Feriolo (Cirla and Scala dei Ratti quarries) and Oltrefiume (Locatelli and Seula quarries). In all of the finds jervisite occurs as radial aggregates of flattened crystals in intimate association with cascandite or in fluffy fibrous aggregates. Specimens in which jervisite forms the peripheral section of divergent aggregates of cascandite are also known. Good quality single crystals of jervisite, such as the one studied by Merlino & Orlandi (2006), are exceptionally rare. As a result, a complete mineralogical characterization of this interesting Sc-bearing pyroxene was not previously possible. During a field excursion to the Seula quarry in August 2017 one of the authors (S.V.) found a specimen exhibiting several divergent groups of exceptionally well-crystallized prisms of jervisite perched on quartz and albite in a miarolitic cavity (Fig. 1). These exceptional crystals, up to 250 μm in length (Fig. 4), allowed for high-quality data collection and refinement of the crystal structure along with characterization of the chemical, optical, and morphological properties of this species.

Chemical Composition

Chemical compositions were obtained with an electron microprobe operated in wavelength dispersive mode (EMP-WDS) in the Earth Sciences Department of the University of Milan. The crystal used for the single-crystal data collection was mounted in epoxy, polished and carbon coated, then analyzed using a JEOL JXA-8200 Superprobe with an accelerating voltage of 15 kV, a beam current of 5 nA, and a beam diameter of 5 μm. Counting times of 30 s on the peak positions and 10 s on the backgrounds were used. The following minerals or synthetic compounds served as standards: grossular for Si, Ca, and Al; rhodonite for Mn; fayalite for Fe; ilmenite for Ti; omphacite for Na; forsterite for Mg; and synthetic $ScPO_4$ for Sc. The raw data were corrected for matrix effects using the protocol implemented in the JEOL suite of programs. The average (seven analysis points) chemical composition of jervisite is presented in Table 1. The empirical formula, normalized on 2 Si *apfu*, is: $(Na_{0.83}Ca_{0.14})_{\Sigma 0.97}(Sc_{0.87}Fe_{0.07}Mn_{0.04}Al_{0.01}Ti_{0.01})_{\Sigma 1.00}Si_2O_{6.00}$, in very good agreement with the general formula of jervisite. The chemical compositions from Mellini *et al.* (1982) and Merlino & Orlandi (2006) are included in Table 1 for comparison.

Optical and Morphological Characters

An aggregate of elongated crystals of jervisite was examined with a polarizing microscope in order to determine the optical properties of this mineral. Individual crystals are approximately 30 μm thick and 400 μm long (Fig. 4A); they are terminated by two faces making an angle of 60°. Interference colors attain yellow of the second order, thus indicating a birefringence of approximately 0.025, assuming a thickness of 30 to 40 μm for the fibers.

The crystals were oriented using the shape model developed with the four-circle diffractometer for absorption corrections. On the (010) section, the crystals show a right extinction with a negative elongation, and an interference figure shows that they are biaxial positive with a high 2V angle. *X* is parallel to the **c** axis, *Y* is parallel to the **b** axis, and *Z* is parallel to the **a** axis. The mineral is colorless, and no dispersion was observed. Refractive indices were measured under sodium light ($\lambda = 589$ nm) and correspond to $\alpha = 1.684(2)$, $\beta = 1.704(6)$, and $\gamma = 1.733(12)$. The calculated 2V angle is 69.2°.

A scanning electron microscope image of the same aggregate of crystals is shown in Figure 4A. Considering the orientation obtained from the single-crystal X-ray diffraction measurements, as well as the angle measurement obtained with the optical microscope, we

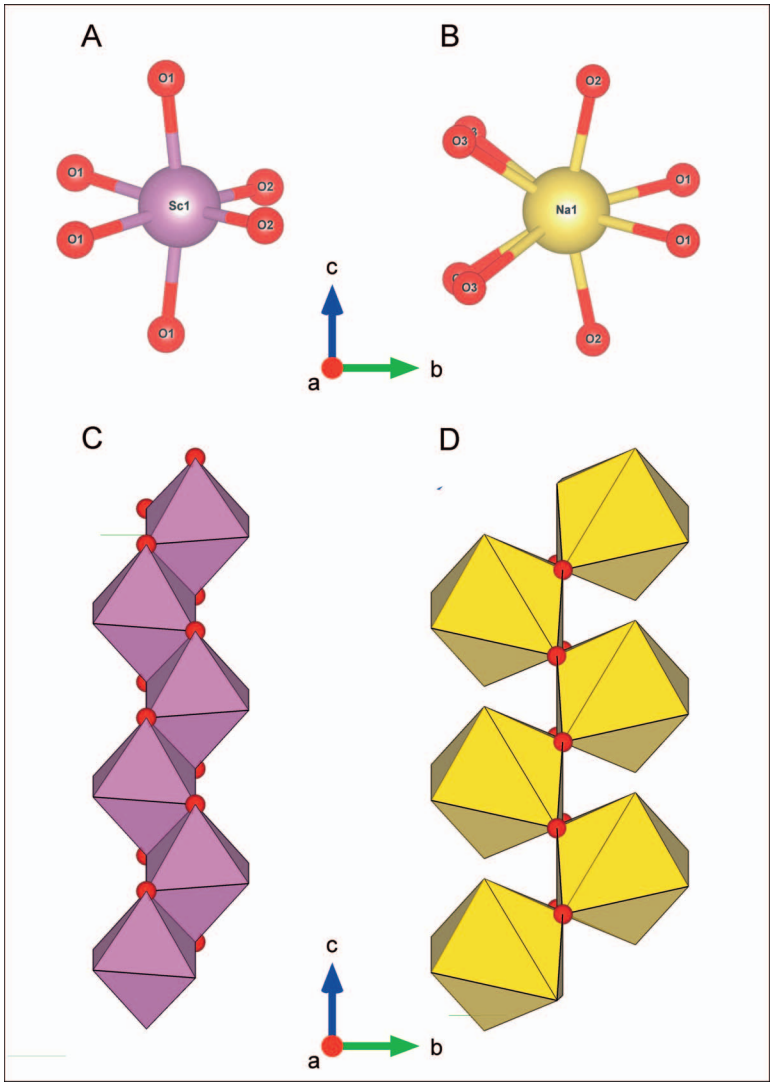

FIG. 2. Jervisite structural features. (A) *M*1 coordination polyhedron; (B) *M*2 coordination polyhedron; (C) the M1 chain; (D) the M2 chain. Violet M1 = Sc, yellow M2 = Na. Drawn using VESTA (Momma & Mizumi 2011).

were able to determine the crystal faces corresponding to this jervisite sample. The crystal model is shown on Figure 4B; it fits the scanning electron microscope image perfectly and indicates the presence of the dominant forms {100} and {010}, associated with less-developed $\{\bar{1}41\}$, $\{22\bar{1}\}$, and {001} faces.

RAMAN SPECTROSCOPY

Raman spectra were obtained with a high-resolution confocal Raman microscope (Renishaw inVia Reflex) equipped with a Leica DM2500 polarizing microscope, a 50× LWD objective, and motorized x–y stages. Spectra were obtained using 532-nm line, solid-state lasers with a power of approximately 10 mW at the sample, in the spectral range 150–1900 cm^{-1}, with a spectral resolution of ± 0.5 cm^{-1} and acquisition time of 2 min (1 s of exposure, with 100% of the laser power and 120 accumulations). An internal standard (silicon wafer at 520.5 cm^{-1}) was used for calibration.

The Raman spectra of jervisite show the characteristic peaks of pyroxene spectra and strongly resemble that of aegirine. Table 2 reports the positions

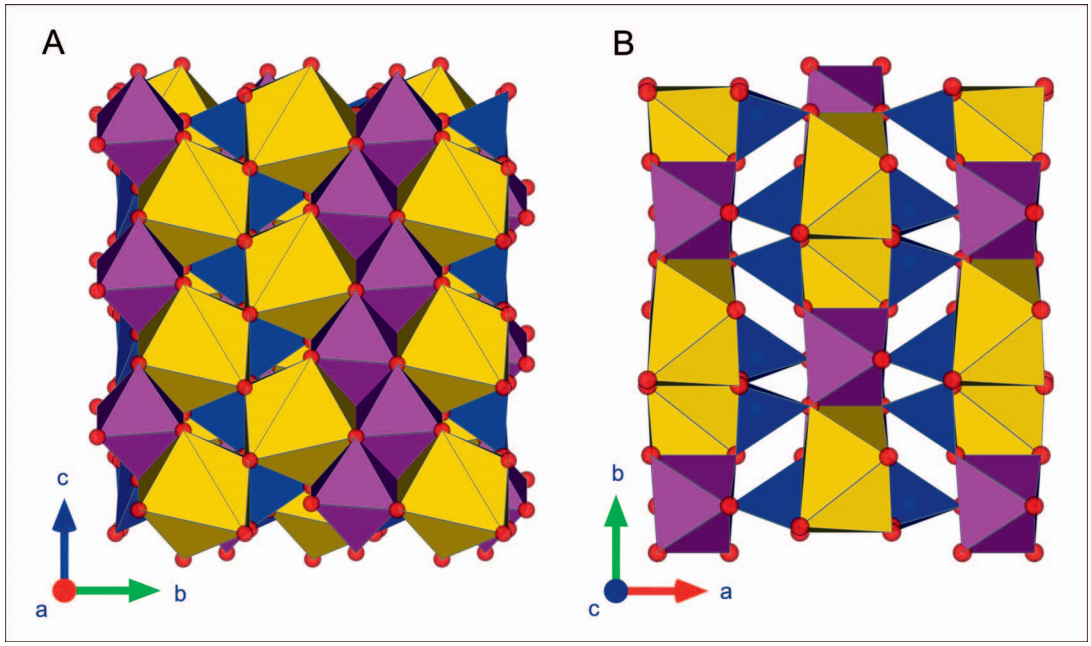

FIG. 3. The crystal structure of jervisite. (A) down **a**, (B) down **c**. Violet M1 = Sc, yellow M2 = Na. Drawn using VESTA (Momma & Mizumi 2011).

of the measured Raman bands for jervisite; a 90° rotation of the crystal with respect to the polarization direction of the laser only produces changes in relative intensities of the peaks (Fig. 5). Table 2 also reports the attribution of the vibrational modes obtained by comparison with other Na pyroxenes (Buzatu & Buzgar 2010) and from the first-principle calculations performed for the Ca-Mg pyroxene diopside (Prencipe *et al*. 2012), whose spectrum shows many similarities with that of jervisite. The main differences are in the high-wavenumber range (900–1100 cm^{-1}), related to Si–O_{nbr} stretching (O_{nbr} = non-bridging oxygens, O_1 and O_2), where the spectrum of jervisite appears to be more complicated. The same differences also occur in the other Na pyroxenes. This can be attributed to the greater difference in behavior between O1 and O2 in jervisite; in diopside O1 and O2 are almost equivalent in terms of Si–O and M–O distances. That means that Si–O1 and Si–O2 stretching vibrations, overlapping in diopside, appear as separate bands in jervisite and in Na pyroxenes. Traditionally (Buzatu & Buzgar 2010), the Raman bands in pyroxene spectra at wavenumbers lower than 390 cm^{-1} are attributed to M–O vibrations; from the first principles calculations on diopside, it appears that even in that spectral range the SiO_4 tetrahedra tilting gives a strong contribution (Prencipe *et al*. 2012). For that reason, in our attribution we consider both M–O vibrations and SiO_4 tetrahedra tilting. Even in the intermediate range (400–600 cm^{-1}), the interpretation offered by calculations which extend the contribution of O–Si–O bending motions toward higher wavenumbers follows the traditional attributions. Even if the Raman spectra of jervisite is similar to those of other Na pyroxenes such as aegirine, jadeite, namansilite, and kosmochlor (Downs 2006), the wavenumbers are characteristic, and the Raman spectrum allows jervisite to be identified in an univocal way.

STRUCTURE REFINEMENT AND DESCRIPTION

Complete single-crystal X-ray diffraction data were collected with an Agilent Technologies Xcalibur 4-circle diffractometer equipped with an EOS CCD-area detector in the Laboratoire de Minéralogie et Cristallochimie of the Earth Science Department, University of Liège, using graphite-monochromatized Mo$K\alpha$ radiation and operated at 50 kV and 40 mA. To maximize the reciprocal space coverage, a combination of omega and phi scans was used, with a step size of 1° and an exposure time per frame of 20 s. A total of 1609 reflections up to a maximum of 28.58° were collected, out of which 540 were unique, giving a metrically monoclinic unit-cell with $a = 9.8478(2)$ Å, $b = 9.0575(1)$ Å, $c = 5.3409(3)$ Å, $\beta = 106.87(2)°$, and $V = 455.89(2)$ $Å^3$ (Table 2). Intensity data were

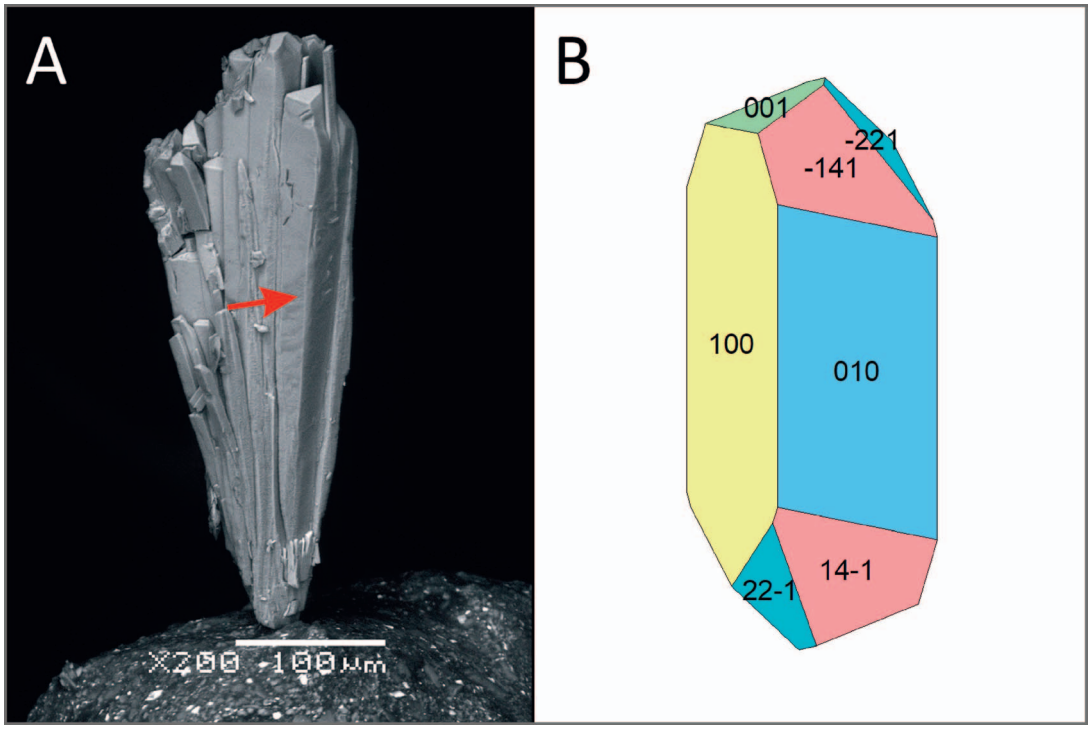

FIG. 4. (A) Back-scattered electron image of the group of jervisite crystals used for optical characterization and morphological study (red arrow indicates the crystal from which the optical indices were measured). (B) Model of jervisite obtained by direct angle measurement, crystallographic orientation using the shape model developed with the four-circle diffractometer, and the BSE-SEM image.

corrected for Lorentz-polarization and absorption effects with the CrysAlis software (Oxford Diffraction 2006). Further details of the data collection of jervisite are given in Table 3.

The crystal structure of jervisite was solved *ab initio* from the single-crystal X-ray intensity data in space group *C*2/*c* after checking for systematic extinctions using the SUPERFLIP program based on the charge-flipping algorithm (Palatinus & Chapuis 2007) and implemented in JANA2006 (Petricek *et al.* 2006). One *M*1, one *M*2, one Si, and three independent O sites were located (Table 4).

The anisotropic structure refinement was performed using the JANA2006 software (Petricek *et al.* 2006). The neutral X-ray scattering curves of Na, Sc, Si, and O were obtained from the International Tables for Crystallography C (Wilson & Prince 1999). Convergence was achieved, and the variance–covariance matrix showed no high correlation (larger than 0.60) among the refined parameters. No peaks larger than +0.56/–0.71 $e^{-}/Å^3$ were present in the final difference-Fourier maps of the electron density. The final agreement index ($R1$) was 0.0412 for 49 refined parameters and 382 unique reflections with $I > 3\sigma(I)$ (Table 2). Atomic coordinates and isotropic displacement parameters are reported in Table 4 (anisotropic displacement parameters, and relevant bond lengths and angles, are listed in Tables D1, D2, and D3, available from the MAC Depository of Unpublished Data[1]; additional data are reported in the deposited .cif file).

The crystal structure of jervisite conforms to the general topology of clinopyroxenes and in particular with the crystal structure of its synthetic analogue (Hawthorne & Grundy 1973) and the specimen from the Prini quarry (adjacent to the Seula quarry) described in Merlino & Orlandi (2006) and reported in the introduction of this paper.

[1] Found on the MAC website at http://www.mineralogicalssociation.ca

TABLE 2. POSITION OF THE MEASURED RAMAN BANDS OF JERVISITE AND THEIR ATTRIBUTIONS

Wavenumber (cm^{-1})	**c** axis parallel to laser polarization	**c** axis perpendicular to laser polarization	Attribution
171.5	m	w	SiO_4 tetrahedra tilting and cations motions
191.5	w	m	
217	w	vw	
227.5	vw	-	
255.5	w	w	
294.5	w	m	SiO_4 tetrahedra tilting (librations)
326.5	m	vs	
358	m	m	
385.5	s	s	
474	vw	-	O–Si–O bending
496.5	m	m	
523.5	m	w	
556	m	m	
622.5	-	vw	
666.5	vs	s	Si–O_{br}–Si bending
742.8	w	w	Si–O_{br} stretching
874	m	m	
934.5	w	w	Si–O_{nbr} stretching
969.5	m	m	
990	s	m	
1025	vs	m	
1093.5	-	vw	

Notes: vw = very weak, w = weak, m = medium, s = strong, vs = very strong.

TABLE 3. DETAILS OF THE DATA COLLECTION AND STRUCTURE REFINEMENT OF JERVISITE

Crystal shape	Irregular prism
Crystal size (μm)	120 × 80 × 70
Crystal color	colorless
T (K)	298
Unit-cell constants	a = 9.8478 (2) Å b = 9.0575 (1) Å c = 5.3409 (3) Å β = 106.87 (2) ° V = 455.89 (2) $Å^3$
Reference chemical formula	$NaScSi_2O_6$
Space Group	$C2/c$
Z	4
Radiation	X-ray Mo$K\alpha$
Wavelength (Å)	0.7107
Diffractometer	Xcalibur
Data-collection method	omega/phi scan
h_{min}, h_{max}	–12/12
k_{min}, k_{max}	–12/11
l_{min}, l_{max}	–7/6
Redundancy	7.507
Measured reflections	1609
Unique reflections	540
Unique refl. with $I > 3\sigma(I)$	382
Parameters (refinement)	49
$R1$ (obs/all) (%)	4.12/6.27
Final $wR2$	4.23/4.58
Residuals ($e^-/Å^3$)	+0.56/–0.71

$R_{int} = \sum|F^2_{obs} - F^2_{obs}(mean)|/\sum(F^2_{obs})$; $R1 = \sum(|F_{obs} - F_{calc}|)/\sum|F_{obs}|$
$wR2 = (\sum(w(F^2_{obs} - F^2_{calc})^2)/\sum(w(F^2_{obs})^2)^{0.5}$, $w = 1/(\sigma^2(F_{obs} + 0.0001F^2_{obs}))$.

Discussion

From the chemical point of view, the jervisite studied in this work is a Sc-bearing Na pyroxene. In particular, it conforms to aegirine in the classification scheme developed in Morimoto *et al*. (1988), since the *M*2 site is populated mainly by Na (83%) and minor Ca (14%) (Fig. 2A and B), whereas the *M*1 site is almost entirely populated by Sc (87.0%) with minor Fe (7.1%) and Mn (4.2%). The chemical composition described here is very close to that reported by Merlino & Orlandi (2006) but is closer to the endmember composition (Table 1). Both these compositions are considerably different from that described by Mellini *et al*. (1982); the difference could be explained by a sub-microscopic mixture of jervisite and cascandite in the specimen studied by Mellini *et al*. (1982) (Table 1). The extremely low amounts of Al, Fe, and Mn in the chemical composition suggest a very low component of jadeite, hedembergite, johannsenite, and namansilite. Therefore, jervisite is defined as the Sc analogue of aegirine with a very low component of hedenbergite, johannsenite, and namansilite, and not of aegirine–augite as described by Mellini *et al*. (1982). The crystal structure of jervisite described in this work conforms almost perfectly with those described by Hawthorne & Grundy (1973) and Merlino & Orlandi (2006). Furthermore, the structure of jervisite is very close to that of synthetic aegirine (Nestola *et al*. 2007). In Table 5 the unit-cell parameters and bond lengths of the *M*1, *M*2, and Si sites of jervisite (from this work and Merlino & Orlandi 2006), synthetic $NaScSi_2O_6$ (Hawthorne & Grundy 1973), synthetic $NaFe^{3+}Si_2O_6$ (aegirine from Nestola *et al*. 2007), and davisite, $CaScAlSiO_6$, a Sc-bearing pyroxene found only in chondritic meteorites (synthetic from Ohashi & Ii 1978, Ma & Rossman 2009), are reported for comparison. All variations of unit-cell parameters, bond distances, and volumes of *M*1 and *M*2 sites in

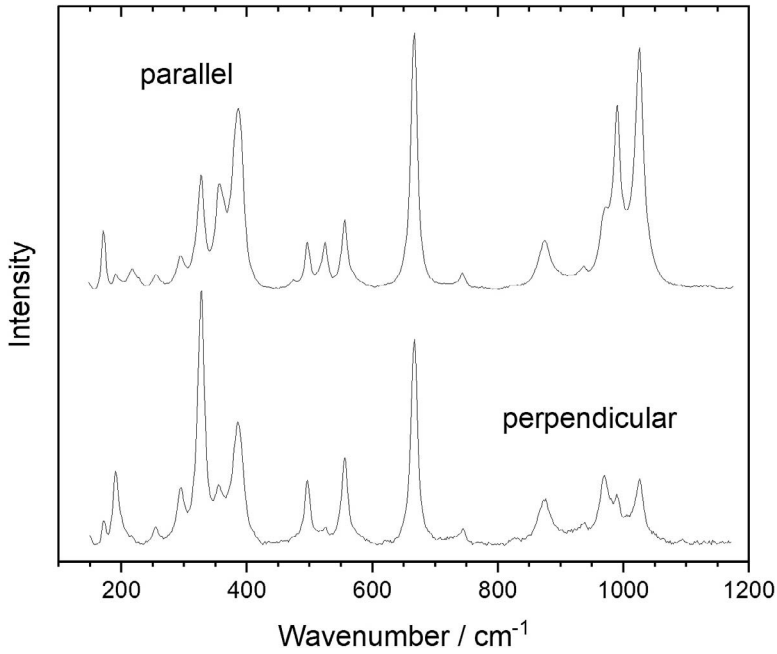

FIG. 5. Raman spectra of jervisite obtained with the **c** axis of the crystal parallel and perpendicular to the laser polarization.

jervisite structures are evidently independent from the chemical composition given the ionic radii of Na = 1.02, Ca = 0.99, Fe = 0.64, and Sc = 0.74 Å (Shannon 1976). In davisite the volume of the *M*2 polyhedron is lower due to the presence of Ca instead of Na, despite a larger unit-cell volume (Table 5). Examination of the distortion indexes, calculated using VESTA (Momma & Mizumi 2011, Table 5), evidences a different and stronger distortion of *M*2 antiprisms occupied by Na in jervisite with respect to those occupied by Ca in davisite. Moreover, the distortion of the *M*2 antiprism appears to be maintained and to be of the same order for the jervisite structures and the synthetic analogue (Hawthorne & Grundy 1973), and for the synthetic analogue of aegirine (Nestola *et al.* 2007). The distortion of the *M*1 polyhedron is almost constant in jervisite, its synthetic analogue, and the synthetic analogues of aegirine and davisite, as shown in Table 5.

The cation distribution described in Merlino & Orlandi (2006) was adopted to result in the empirical formula. The proper distribution of elements is evidenced by the bond-valence values reported in Table 6 and calculated respecting the effective cation distribution. Moreover, the electron densities of the *M*1 and *M*2 sites obtained from the structure refinement and from the empirical formula are very similar (*M*1: 21.36 and 21.44 e^-, respectively; *M*2: 11.53 and 11.93 e^-, respectively). The measured refractive indices were used to determine a Gladstone-Dale compatibility index of 0.0007 (calculated from the density obtained from the chemical composition and single-crystal unit-cell parameters and from the measured average refractive index). This compatibility index is superior (Mandarino 1981).

TABLE 4. REFINED POSITIONAL AND THERMAL DISPLACEMENT PARAMETERS (Å^2) OF JERVISITE AT 298 K

Site	Element	Refined occupancy	*x*	*y*	*z*	U_{iso}/U_{eq}
*M*1	Sc	1.017(5)	0	0.8972(1)	0.25	0.0094(4)
*M*2	Na	1.048(8)	0	0.3040(3)	0.25	0.0191(10)
Si	Si	1	0.2909(1)	0.0878(1)	0.2432(2)	0.0104(4)
O1	O	1	0.1181(3)	0.0795(3)	0.1464(5)	0.0107(10)
O2	O	1	0.3600(3)	0.2472(3)	0.3095(6)	0.0141(11)
O3	O	1	0.3495(3)	0.0093(3)	0.0152(6)	0.0130(11)

TABLE 5. COMPARISON BETWEEN CRYSTALLOGRAPHIC CHARACTERISTICS OF JERVISITE, ITS SYNTHETIC ANALOGUE, AND SYNTHETIC ANALOGUES OF AEGIRINE AND DAVISITE

Mineral	jervisite			aegirine	davisite
Provenance	Baveno, Seula quarry	Baveno, Prini quarry	synthetic	synthetic	synthetic
Reference	This work	Merlino & Orlandi (2006)	Hawthorne & Grundy (1973)	Nestola *et al.* (2007)	Ohashi & Li (1978)
a (Å)	9.8478(2)	9.844(2)	9.8438(4)	9.6623(4)	9.884(2)
b (Å)	9.0575(1)	9.059(2)	9.0439(4)	8.800(2)	8.988(1)
c (Å)	5.3409(3)	5.328(2)	5.3540(2)	5.2956(3)	5.446(1)
β (°)	106.87(2)	106.55(2)	107.215(2)	107.579(3)	105.86(1)
Vol (Å^3)	455.89(2)	455.45	455.31	429.25(3)	465.43
			*M*1 octahedron distances (Å)		
*M*1–O1ii, O1iii	2.182(3) ×2	2.180(5) ×2	2.183(2) ×2	2.113(1) ×2	2.182(1)
*M*1–O1iv, O1v	2.109(3) ×2	2.111(5) ×2	2.105(5) ×2	2.031(1) ×2	2.105(1)
*M*1–O2vi, O2vii	2.025(3) ×2	2.038(5) ×2	2.017(2) ×2	1.939(2) ×2	2.019(1)
Mean	2.105	2.110	2.102	2.028	2.102
Volume (Å^3)*	12.2781		12.2009	10.9401	12.2274
Distortion index*	0.02539		0.02687	0.02923	0.02625
Occupancy Sc (%)	87	85	100	100	100
			*M*2 antiprism distances (Å)		
*M*2–O1, O1viii	2.483(4) ×2	2.495(5) ×2	2.490(2) ×2	2.446(2) ×2	2.447
*M*2–O2ix, O2x	2.402(3) ×2	2.387(5) ×2	2.411(6) ×2	2.369(2) ×2	2.387
*M*2–O3vi, O3vii	2.480(4) ×2	2.472(5) ×2	2.490(2) ×2	2.388(2) ×2	2.543
*M*2–O3xi, O3xii	2.878(4) ×2	2.845(5) ×2	2.894(6) ×2	2.857(2) ×2	2.677
Mean	2.561	2.550	2.544	2.515	2.513
Volume (Å^3)	27.6920		27.7905	26.1213	26.4592
Distortion index*	0.06192		0.06436	0.06795	0.03849
Element	Na	Na	Na	Na	Ca
Occupancy (%)	83	78	100	100	100
			Si tetrahedron distances (Å)		
Si–O1	1.631(3)	1.623(4)	1.630(3)	1.628(1)	1.690(1)
Si–O2	1.591(3)	1.590(5)	1.592(2)	1.598(2)	1.663(1)
Si–O3	1.652(4)	1.659(5)	1.653(2)	1.638(1)	1.707(1)
Si–O3i	1.652(3)	1.663(5)	1.653(3)	1.646(1)	1.721(1)
Mean	1.632	1.634	1.632	1.628	1.695

Notes: * calculated using VESTA (Momma & Mizumi 2011).

TABLE 6. BOND VALENCE FOR JERVISITE

	*M*1	*M*2	Si	Sum
O1	0.413 (×2)	0.159	0.975	1.96
		0.159		
	0.484 (×2)			
O2	0.583	0.193	1.083	1.859
	0.583	0.193		
O3		0.161	0.933	2.084
		0.062	0.928	
Sum	2.96	0.927	3.919	

Notes: *M*2 is calculated with Na 0.94 + Ca 0.06 contributions as per the structure refinement.

Acknowledgments

The authors are grateful to Associate Editor Jan Cempírek and two anonymous reviewers for their valuable suggestions. The Raman spectra were collected in the Laboratory for Provenance studies (DISAT), part of the Project MIUR – Dipartimenti di Eccellenza 2018–2022. Italo Campostrini is thanked for the BSE image of jervisite. Andrea Risplendente is thanked for help during the EMP analyses.

References

Artini, E. (1915) Due minerali di Baveno contenenti terre rare: weibyeïte e bazzite. *Rendiconti dell'Accademia dei Lincei* **24**, 313–319.

Buzatu, A. & Buzgar, N. (2010) The Raman study of single-chain silicates. *Analele Stiintifice de Universitatii "AI Cuza din" Iaşi, Geologie* **LVI-1**, 107–125.

Demartin, F., Gramaccioli, C.M., & Pilati, T. (2000) Structure refinement of bazzite from pegmatitic and miarolitic occurrences. *Canadian Mineralogist* **38**, 1419–1424.

Downs, R.T. (2006) The RRUFF Project: an integrated study of the chemistry, crystallography, Raman and infrared spectroscopy of minerals. Program and Abstracts of the 19th General Meeting of the International Mineralogical Association in Kobe, Japan, O03–13.

Gramaccioli, C.M., Campostrini, I., & Demartin, F. (2004) Scandium minerals in the miaroles of granite at Baveno, Italy. *European Journal of Mineralogy* **16**, 951–956.

Guastoni, A. & Pezzotta, F. (2004) Kristiansenite a Baveno, secondo ritrovamento mondiale della specie. *Rivista Mineralogica Italiana* **30**, 247–251.

Hawthorne, F.C. & Grundy, H.D. (1973) Refinement of the crystals structure of $NaScSi_2O_6$. *Acta Crystallographica* **B29**, 2615–2616.

Ito, J. & Frondel, C. (1968) Syntheses of the scandium analogues of aegirine, spodumene, andradite and melanotekite. *American Mineralogist* **53**, 1276–1280.

Ma, C. & Rossman, G.R. (2009) Davisite, $CaScAlSiO_6$, a new pyroxene from the Allende meteorite. *American Mineralogist* **94**, 845–848.

Mandarino, J.A. (1981) The Gladstone-Dale relationship: part IV. The compatibility concept and its application. *Canadian Mineralogist* **19**, 441–450.

Mellini, M., Merlino, P., & Orlandi, P. (1982) Cascandite and jervisite, two new scandium silicates from Baveno, Italy. *American Mineralogist* **67**, 599–603.

Merlino, S. & Orlandi, P. (2006) Jervisite, Na Sc Si_2O_6: a new occurrence, chemical data and crystal structure. *Periodico di Mineralogia* **75**, 189–194.

Momma, K. & Mizumi, F. (2011) VESTA 3 for three-dimensional visualization of crystal, volumetric and morphology data. *Journal of Applied Crystallography* **44**, 1272–1276.

Morimoto, N., Fabries, J., Ferguson, A.K., Ginzburg, I.V., Ross, M., Seifert, F.A., Zussman, J., Aoki, K., & Gottardi, G. (1988) Nomenclature of pyroxenes. *American Mineralogist* **75**, 1123–1173.

Nestola, F., Tribaudino, M., Boffa Ballaran, T., Liebske, C., & Bruno, M. (2007) Crystal structure of pyroxenes along the jadeite-hedembergite and jadeite-aegirine joins. *American Mineralogist* **92**, 1492–1501.

Ohashi, H. & Ii, N. (1978) Structure of calcium scandium aluminum silicate ($CaScAlSiO_6$)-pyroxene. *Journal of the Japanese Association of Mineralogists, Petrologists and Economic Geologists* **73**, 267–273.

Orlandi, P. (1990) Zibaldone di mineralogia italiana. *Rivista Mineralogica Italiana* **14**, 137–144.

Orlandi, P., Pasero, M., & Vezzalini, G.(1998) Scandiobabingtonite, a new mineral from the Baveno pegmatite, Piedmont, Italy. *American Mineralogist* **83**, 1330–1334.

Oxford Diffraction (2006) *CrysAlis CCD* and *CrysAlis RED*. Oxford Diffraction Limited, Abingdon, Oxfordshire, England.

Palatinus, L. & Chapuis, B. (2007) *SUPERFLIP* – a computer program for the solution of crystal structures by charge flipping in arbitrary dimensions. *Journal of Applied Crystallography* **40**, 786–790.

Petricek, V., Dusek, M., & Palatinus, L. (2006) *JANA2006*. Institute of Physics, Czech Academy of Sciences, Prague, Czech Republic.

Potter, E.G. & Mitchell, R.H. (2005) Mineralogy of the Deadhorse Creek volcaniclastic breccia complex, northwestern Ontario, Canada. *Contributions to Mineralogy and Petrology* **150**, 212–229.

Prencipe, M., Mantovani, L., Tribaudino, M., Bersani, D., & Lottici, P.P. (2012) The Raman spectrum of diopside: a comparison between ab initio calculated and experimentally measured frequencies. *European Journal of Mineralogy* **24**, 457–464.

Shannon, R.D. (1976) Revised effective ionic radii and systematic studies of interatomie distances in halides and chaleogenides. *Acta Crystallographica* **A32**, 751–767.

Wilson, A.J.C. & Prince, E. (1999) *International Tables for X-ray Crystallography, Volume C: Mathematical, physical and chemical tables*. 2nd Edition, Kluwer Academic, Dordrecht, Netherlands.

Received February 15, 2019. Revised manuscript accepted April 18, 2019.